A Supplementary Material

Quantitative assignment of reaction directionality in constraint-based models of metabolism: Application to *Escherichia coli*

R.M.T. Fleming[1], I. Thiele, H.P. Nasheuer

A.1 Metabolite species standard Gibbs energy of formation

A.1.1 Measurement of apparent equilibrium constants

The standard Gibbs energy of formation of a metabolite species can, in principal, be calculated by measuring the change required to inorganically synthesize it from its elements in standard state. This is difficult or impossible for large complicated organic metabolites. Alternatively, if a reactant occurs in a reaction where only one reactant standard Gibbs energy of formation is unknown, it is possible to back-calculate this unknown indirectly by measuring the apparent equilibrium constant for the reaction. Consider the biochemical reaction catalyzed by glucose-6-phosphate isomerase, *PGI*.

$$F6P \rightleftharpoons G6P \tag{4}$$

This is an isomerisation between the reactants fructose-6-phosphate, F6P, and glucose-6-phosphate, G6P. At physiological pH, fructose-6-phosphate is distributed between two forms, $F6P^{-2}$ and $F6P^{-1}$, that differ by one hydrogen ion

$$F6P^{-1} \rightleftharpoons F6P^{-2} + H^{+}$$

Likewise, glucose-6-phosphate is distributed between two charged forms, $G6P^{-2}$ and $G6P^{-1}$. The apparent equilibrium constant for biochemical reaction 4 is given by

$$K' = \frac{[G6P]_{eq}}{[F6P]_{eq}} = \frac{\left[G6P^{-1}\right] + \left[G6P^{-2}\right]}{[F6P^{-1}] + [F6P^{-2}]}$$

which is a function of temperature, pressure, pH, ionic strength and the pKa of both weak acids. The apparent equilibrium constant of a reaction, K', is related to the standard transformed reaction Gibbs energy by

$$-RT \ln (K') = \Delta_r G'^{0} \tag{5}$$

Therefore, each time an apparent equilibrium constant is measured, one unknown reactant standard transformed Gibbs energy of formation can be back calculated. This back calculation process is discussed in detail by Alberty [29, 30]. Any error in the measurement of the apparent equilibrium constant is ameliorated in the estimation of reactant standard Gibbs energy of formation by virtue of the logarithmic function in Eq. 5.

A.1.2 Group contribution methodology

There are many reactants for which experimentally derived metabolite species standard Gibbs energies of formation are not available. However, it is possible to estimate standard metabolite species Gibbs energy of formation using a group contribution approach [31, 32]. Briefly, this method considers the thermodynamic properties of each metabolite species as the sum of the properties of its constituent structural subgroups. The standard Gibbs energy of formation of various structural subgroups are estimated by linear regression from experimentally known metabolite species structures, and their standard Gibbs energies of formation. To estimate the standard Gibbs energy of formation for an unknown metabolite species, the contributions of each of its structural subgroups are summed along with an origin term. Henry *et al.*[19, 20] have successfully used this approach to computationally estimate standard Gibbs energy of formation for the majority of metabolite species in *E. coli*. The data input to the algorithm which estimates the standard Gibbs energy of formation is structure files which hold information about the atoms, bonds, connectivity and coordinates of substrate and product molecules [31].

A difficult task in estimating the group contribution of a metabolite species standard Gibbs energy of formation, is the uncertainty due to non-additivity of subgroup contributions. A group contribution is said to be additive

[1]Corresponding author. Address: Science Institute & Center for Systems Biology, University of Iceland. Tel.:+354-618-6245

if the magnitude of the contribution is doubled when the number of such a group in a metabolite species is doubled. Individually, the uncertainty associated with estimation of a particular subgroup standard Gibbs energy of formation is typically small relative to metabolite species standard Gibbs energy of formation. However, for complex metabolites with many subgroups, the combined uncertainty in metabolite species standard Gibbs energy of formation can be significant. Jankowski *et al.* [31] have recently reported a significant improvement to the group contribution methodology, that has reduced the uncertainty and has provided better estimates of metabolite species standard Gibbs energy of formation. They explicitly propagate the uncertainty in subgroup estimates, and provide a standard error, $SE_{\Delta_f G^0_{est,i}}$, for each estimated metabolite species standard Gibbs energy of formation, $\Delta_f G^0_{est,i}$, e.g., Supplementary Table 3.

We take into account the uncertainty in estimated metabolite species standard Gibbs energy of formation when making quantitative assignment of reaction directionality, by estimating minimum and maximum reaction standard Gibbs energy using

$$\begin{aligned} \Delta_r G^0_{min,k} &\equiv \inf\{\mathbf{S}_k^T \cdot (\Delta_f \mathbf{G}^0_{est} \pm \mathbf{SE}_{\Delta_f G^0_{est}})\} \\ \Delta_r G^0_{max,k} &\equiv \sup\{\mathbf{S}_k^T \cdot (\Delta_f \mathbf{G}^0_{est} \pm \mathbf{SE}_{\Delta_f G^0_{est}})\} \end{aligned}$$

where inf denotes the infimum and sup denotes the supremum. Group contribution estimates of metabolite species standard Gibbs energy of formation are based on a reference temperature of $298.15K$ [31]. Standard enthalpy of formation is not available for the majority of *E. coli* metabolite species, and therefore standard Gibbs energy of formation cannot be adjusted to $310.15K$ as described in Section A.5. However, the charge and number of hydrogen atoms in each metabolite species are known. Therefore, we can compute estimates for metabolite species standard transformed Gibbs energy of formation, $\Delta_f G'^0_{est}$, at *in vivo* ionic strength and pH. See Section A.3 and A.4, respectively. Similarly, we can estimate minimum and maximum reaction standard Gibbs energy, $\Delta_r G'^0_{min}$ & $\Delta_r G'^0_{max}$. The group contribution approach represents a valuable complementary approach to the estimation of metabolite species standard transformed Gibbs energy of formation, when such data is not available due to a dearth of experimentally measured equilibrium constants. This is the case for the majority of metabolite species in the *E. coli* genome scale model. Jankowski et al [31] continue to expand the number of different structural groups within the scope of the group contribution method, so we can expect the number of metabolite species without group contribution estimates to continue to shrink.

A.2 Reactant standard transformed Gibbs energy of formation

Chemical potential is a thermodynamic potential introduced by J. Willard Gibbs [62], and can be intuitively thought of as a measure of "the tendency of a substance to change its location, chemical composition or state of aggregation" [63]. In a chemical reaction, a difference in chemical potential between substrates and products represents a driving force for spontaneous change of location, chemical composition or state of aggregation. This is discussed further in Section 2.1. First we discuss chemical potential, from which change in chemical potential can be derived.

Since it is not possible to measure an absolute value for the chemical potential of a metabolite species [64], we follow established nomenclature [65] and use the (molar) Gibbs energy of formation of a metabolite species, $\Delta_f G_j$. The chemical potential of a metabolite species is an intensive quantity, meaning that it does not depend on the absolute number of molecules of that metabolite in a system. In contrast, the Gibbs energy of a metabolite species is an extensive quantity which is given by the product of metabolite species chemical potential and the number of metabolite species. The molar Gibbs energy of a metabolite species is an intensive property since it is the Gibbs energy per mole of metabolite species. Depending on the strictness of convention, one may observe molar Gibbs energy and the chemical potential being used interchangeably.

A.3 *In vivo* ionic strength

In water, many metabolite species dissociate into anions$^-$ and cations$^+$. However, a charged metabolite species in solution does not behave ideally, even at very low concentrations in the physiological range of ionic strength [41]. This is mainly due to attraction of metabolite species with opposite charges, which has the effect of shielding the repulsion between metabolite species of like charge, see Chapt. 26 [66]. At non-zero ionic strength, metabolite species molar Gibbs energy of formation, $\Delta_f G_j$, is given by

$$\Delta_f G_j = \Delta_f G^o_j + RT \ln(a_j) \tag{6}$$

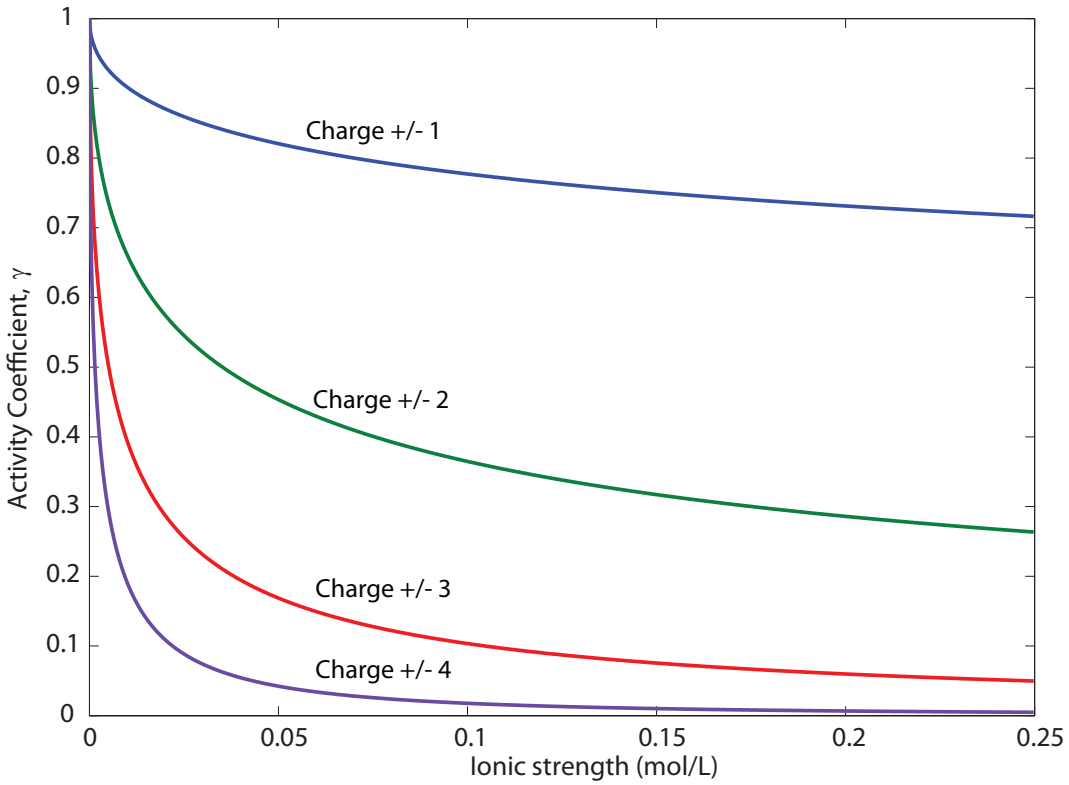

Figure 5: The dimensionless activity coefficient, γ, as a function of ionic strength, I, for metabolite species with different absolute charge, $|z|$. All else being equal, the activity coefficient is the same for a given positive or negative charge of the same magnitude, since z^2 appears in the function giving ionic strength. The activity coefficient of a metabolite species with a charge of either +4 or -4 may differ markedly from 1. This is significant for a number of reactants, such as for D-Fructose-1-6-bisphosphate, NADPH or ATP. e.g. at 0.25 M, & 310.15K, the reactant D-Fructose-1-6-bisphosphate, is distributed between three dissociated forms, FDP^{4-}, $FDP^{3-}$and FDP^{2-}. However, the mole fraction of $FDP^{4-}$is greater than 0.99 with an activity coefficient of 4.8×10^{-3}. This means that a micromolar cytoplasmic concentration of FDP^{4-} actually corresponds to a nanomolar activity.

where R is the gas constant, T is temperature, and a_j is metabolite species activity [41]. The activity of a metabolite species is related to its concentration by $a_j = \gamma_j x_j$, where the activity coefficient, γ_j, represents the non-ideal electrolyte behavior. Given the electric charge of a metabolite species, z_j, one can reasonably approximate the *in vivo* activity coefficient using the extended Debye-H*ü*ckel equation [41] relating charge, z_j, and ionic strength, I, to the activity coefficient

$$\ln(\gamma_j) = -\frac{Az_j^2 I^{\frac{1}{2}}}{1 + BI^{\frac{1}{2}}} \tag{7}$$

where A and B are empirically fitted parameters, which approximate experimentally measured activity coefficients [2]. The ionic strength, I, of a solution is defined by

$$I \equiv \frac{1}{2}\sum_{j=1}^{m} z_j^2 x_j$$

where z_j is the charge, and $x_j$is the concentration of metabolite species j. The *in vivo* ionic strength is thus a function of all charged metabolite concentrations, which are largely unknown [48].

Estimation of activity coefficient using extended Debye-H*ü*ckel equation is considered to be valid in the ionic strength range 0-0.35M [29]. By estimating the activity coefficient for each metabolite species, this term may then be absorbed into Eq. 6 for metabolite species Gibbs energy of formation

$$\begin{aligned} \Delta_f G_j &= \Delta_f G_j^o + RT\ln a_j \\ &= \Delta_f G_j^o + RT\ln(\gamma_j x_j) \\ &= \Delta_f G_j^o + RT\ln\gamma_j + RT\ln x_j \\ &\equiv \Delta_f G_j^0 + RT\ln x_j \end{aligned} \tag{8}$$

We shall still refer to $\Delta_f G_j^0$ as a metabolite species standard Gibbs energy of formation but the slight change in superscript, from ^{o} to ^{0}, is used to remind the reader that it is now a function of ionic strength. By absorbing the activity coefficient into the standard term we retain the convenience of dealing with experimentally measured concentrations and not activities [29]. Obviously, it would be of significant benefit to have experimental data on typical values of the actual *in vivo* ionic strength. Unless otherwise specified, we assume an ionic strength of 0.25 M.

A.4 *In vivo* pH

The second law of thermodynamics dictates that net spontaneous change must be in the direction of a drop in thermodynamic potential. When modeling the thermodynamics of any system, the set of variables that are held constant dictate the appropriate thermodynamic potential [41]. At constant temperature and pressure, the appropriate thermodynamic potential is Gibbs energy. In biochemical thermodynamics, we must also consider that the buffering capacity of intracellular proteins acts as a bath which maintains a constant pH. At constant temperature, pressure and pH, the appropriate thermodynamic potential is the transformed Gibbs energy [29]. The adjective refers to the Legendre transformation which is used to account for the fact that pH is a specified constant. This transformation can be made directly to the standard Gibbs energy of formation, giving rise to the definition of the standard transformed Gibbs energy of a metabolite species

$$\triangle_f G_j'^0 \equiv \triangle_f G_j^0 - N_j(H)\Delta_f G(H^+) \tag{9}$$

where $N_j(H)$ is the number of hydrogen atoms in metabolite species j and $\Delta_f G(H^+)$ is the hydrogen ion Gibbs energy of formation. It is important to realise that hydrogen ion Gibbs energy of formation is a function of ionic strength and temperature, just like any other metabolite species, see Eq. 7 and Eq. 8. For a comprehensive treatment of Legendre transforms in biochemical thermodynamics, see Alberty [67, 29, 30].

[2] $B = 1.6L^{-\frac{1}{2}}mol^{-\frac{1}{2}}$. A is a function of temperature and pressure, at $298.15K$ and atmospheric pressure, then $A = 0.510651L^{-\frac{1}{2}}mol^{-\frac{1}{2}}$.

A.5 *In vivo* temperature

The enthalpy, H, is a thermodynamic potential defined by a Legendre transformation of the internal energy

$$H \equiv U + PV \tag{10}$$

Only at constant pressure, the differential of enthalpy provides the appropriate criterion for spontaneous change. Metabolite species standard Gibbs energy of formation may be estimated as a function of temperature, $\triangle_f G_j^o(T)$, using

$$\triangle_f G_j^o(T) = \left(\frac{T}{298.15K}\right) \triangle_f G_j^o(T = 298.15K) + (1 - \frac{T}{298.15K}) \triangle_f H_j^o(T = 298.15K) \tag{11}$$

where $\triangle_f G_j^o(T = 298.15K)$ and $\triangle_f H_j^o(T = 298.15K)$ are metabolite species standard Gibbs energy of formation and metabolite species standard enthalpy of formation, respectively, measured at 298.15K [29]. Metabolite species standard enthalpy of formation may be obtained from calorimetric experiments [29] and it also may be a function of temperature but we assume here that this variation is small going from $298.15K \rightarrow 310.15K$.

Additional effects of temperature on Gibbs energy of formation arise due to the temperature dependence of the parameter A in the extended Debye-H*ü*ckle equation 7 used for predicting metabolite species activity coefficient. This is particularly important when estimating the activity of hydrogen ions at a specified pH. The effect of temperature on hydrogen ion activity appears as an adjustment to the hydrogen ion Gibbs energy of formation. This temperature effect on hydrogen ion Gibbs energy of formation will then be multiplied by the number of hydrogen atoms in each metabolite species when making a Legendre transformation for constant pH, as in Eq. 9.

A.6 Combined equation for ionic strength, pH and temperature adjustment

Amalgamation of all the adjustments to metabolite species standard Gibbs energy of formation, $\triangle_f G_j^o$, for specified temperature (Eq. 11), specified ionic strength (Eq. 8), and specified pH (Eq. 9) gives a metabolite species standard transformed Gibbs energy of formation as

$$\Delta_f G_j'^0 = \left(\frac{T}{298.15}\right) \triangle_f G_j^o + (1 - \frac{T}{298.15}) \triangle_f H_j^o - \frac{RTAz_j^2 I^{\frac{1}{2}}}{1 + BI^{\frac{1}{2}}} - N_j(H)\Delta_f G(H^+)$$

This equation highlights that the metabolite species standard transformed Gibbs energy of formation depends on properties that are specific to that metabolite species.

A.7 Concentrations of water and dissolved gases

In the treatment of biochemical reactions, as in this study, it is typical to assume an activity of water equal to one [68]. In addition, we use the dissolved oxygen (reactant) concentration range, $0.1 - 8.6 \times 10^{-6}$ M . In aqueous phase the reactant carbon dioxide is distributed between a number of metabolite species, some involving water $[CO_2] = [CO_2(aq)] + [CO_3^{2-}] + [HCO_3^-] + [H_2CO_3]$. We assumed a carbon dioxide (reactant) concentration of $[CO_2] = 1$ mM [20]. The details follow the special thermodynamic treatment of carbon dioxide as described by Alberty, (Section 8.7 in [29]).

A.8 Qualitative assignment of reaction directionality

During reconstruction of a biochemical network, qualitative assignment of reaction directionality is made on a reaction-by-reaction basis using various forms of evidence from biochemical characterization experiments of specific enzymes [2]. If, at physiological concentrations of substrates and products, a reaction is experimentally observed to favor the production of products then it may be classified as irreversible in a forward direction. If biochemical characterization is not available, a qualitative assignment of reaction irreversibility can be made if a reaction is co-factor coupled, such as to the hydrolysis of ATP, since ATP driven reactions tend to be effectively irreversible.

Reaction	E.C. / Gene	Eq. & qualitative direction	$\Delta_r G'^0_{low}$	$\Delta_r G'^0_{high}$	$\Delta_r G'_{min}$	$\Delta_r G'_{max}$
D-Erythrose-4-phosphate dehydrogenase*	1.2.1.72	**e4p** + h2o + nad ⇌ **4per** + 2 h + nadh	-66.4	-51.1	-105.6	-11.9
galactokinase	2.7.1.6	atp + gal ⇌ adp + gal1p + h	-49.0	-49.0	-88.2	-9.8
γ-glutamyl γ-aminobutyric acid dehydrogenase	puuC	**ggbutal** + h2o + nadp ⇌ **gg4abut** + 2 h + nadph	-71.8	-43.5	-111.0	-4.3
glutathione oxidoreductase	1.8.1.7	gthox + h + nadph ⇌ 2 gthrd + nadp	-914.0	-914.0	-982.9	-884.9
IMP cyclohydrolase*	3.5.4.10	h2o + imp ⇌ **fprica**	-60.1	-26.4	-79.7	-6.7
phosphoribosylpyrophosphate synthetase	2.7.6.1	atp + r5p ⇌amp + h + **prpp**	-43.3	-43.3	-82.5	-4.1
phosphate reversible transport via symport periplasm	pitA or pitB	h[p] + pi[p] ⇌ h + pi	8.5	8.5	6.7	26.3
glycogen phosphorylase (GLCP)	2.4.1.1	**glycogen** + pi → g1p	693.0	794.0	685.3	825.5
glycogen phosphorylase (GLCP2)	2.4.1.1	**bglycogen** + pi → g1p	693.0	794.0	685.3	825.5
2-C-methyl-D-erythritol-2-4-cyclodiphosphate synthase*	4.6.1.12	**2p4c2me** → **2mecdp** + **cmp**	63.8	167.2	14.5	176.7
methionine adenosyltransferase*	2.5.1.6	atp + h2o + met-L → **amet** + pi + ppi	114.6	176.1	63.5	203.5
phosphoribosylaminoimidazole synthase*	6.3.3.1	atp + **fpram** → adp + **air** + 2 h + pi	84.7	156.2	33.7	183.5

Table 2: Reactions, as given in the iAF1260 reconstruction, with quantitatively assigned reaction directions that are more constrained, or reversed, in comparison with qualitative assignments. The * denotes reactions that, contrary to quantitative assignment, are essential in the forward direction, for aerobic growth on glucose minimal medium. The key to reactant abbreviations is given in Table 3. The **bold** reactant abbreviations denote the use of group contribution estimates where data back calculated from equilibrium constants was not available. Where appropriate, the low and high standard transformed reaction Gibbs energy, $\Delta_r G'^0_{low}$ and $\Delta_r G'^0_{high}$, account for a one standard deviation uncertainty in reactant group contribution estimates. The minimum and maximum transformed reaction Gibbs energy, $\Delta_r G'_{min}$ and $\Delta_r G'_{max}$, also assume a $0.01-20\,mM$ physiological reactant concentration range, except: $[CO_2] = 10^{-4}\ M$, $[H_2O] = 1\ M$, and $[O_2] = 8.2 \times 10^{-8} - 8.2 \times 10^{-6}\ M$. Data given for a temperature of $310.15\ K$, ionic strength of $0.25\ M$, and pH of 7.7. See Supplementary Table 3 for metabolite legend.

A.9 Quantitative tightening of qualitatively assigned reaction directionality: reconciliation with experimental literature

A.9.1 Qualitatively reversible yet quantitatively forward

Erythrose 4 phosphate dehydrogenase (E.C. 1.2.1.72) D-Erythrose-4-phosphate dehydrogenase catalyzes the first step in the biosynthesis of essential coenzyme pyridoxal 5'-phosphate (active vitamin B6), from the pentose phosphate precursor, D-erythrose-4-phosphate [69]

$$\text{D-Erythrose-4-phosphate+NA}D^{+}\text{+}H_2\text{O} \rightleftharpoons \text{4-Phosphoerythronate+2h+NADH}$$

In silico, the forward oxidation reaction direction is essential for growth on glucose minimal medium. Biochemical characterisation experiments established that, at pH 7, the oxidation of 1 mM D-Erythrose-4-phosphate and reduction of 1 mM NAD^+ proceeded to completion, upon addition of D-Erythrose-4-phosphate dehydrogenase as measured by NADPH production [70]. This suggests that indeed the D-Erythrose-4-phosphate dehydrogenase reaction is strongly thermodynamically favorable, supporting the quantitative assignment.

Abbr	Metabolite	$\pm SE_{\Delta_f G^0_{est}}$
2mecdp	2-C-methyl-D-erythritol-2-4-cyclodiphosphate	18.4
2p4c2me	2-phospho-4-cytidine-5-diphospho-2-C-methyl-D-erythritol	17.3
4per	4-Phospho-D-erythronate	3.8
air	5-amino-1-5-phospho-D-ribosyl-imidazole	16.4
amet	S-Adenosyl-L-methionine	30.8
bglycogen	branching-glycogen	50.5
cmp	Cytidine-5'-monophosphate	16.0
e4p	D-Erythrose-4-phosphate	3.9
fpram	2-Formamido-N1-5-phospho-D-ribosyl-acetamidine	19.4
fprica	5-Formamido-1-5-phospho-D-ribosyl-imidazole-4-carboxamide	16.9
g1p	D-Glucose-1-phosphate	-
gal1p	alpha-D-Galactose-1-phosphate	-
gal	D-Galactose	-
gg4abut	gamma-glutamyl-gamma-aminobutyric-acid	7.1
ggbutal	gamma-glutamyl-gamma-butyraldehyde	7.1
glycogen	glycogen	50.5
gthox	Oxidized-glutathione	-
gthrd	Reduced-glutathione	-
imp	Inosine monophosphate	-
met-L	L-Methionine	-
nad	Nicotinamide-adenine-dinucleotide	-
nadh	Nicotinamide-adenine-dinucleotide–reduced	-
nadp	Nicotinamide-adenine-dinucleotide-phosphate	-
nadph	Nicotinamide-adenine-dinucleotide-phosphate–reduced	-
nmn	Nicotinamide ribonucleotide	-
pi	Phosphate	-
ppi	Diphosphate	-
prpp	5-Phospho-alpha-D-ribose-1-diphosphate	-
r5p	alpha-D-Ribose-5-phosphate	-

Table 3: Reactants involved in reactions with quantitatively assigned directions that are more constrained, or reversed, as compared with qualitatively assigned direction (Reactions given in Supplementary Table 2). The reactants where group contribution estimates were used are indicated with the associated standard error in standard Gibbs energy of formation, $SE_{\Delta_f G^0_{est}}$, [31].

Galactokinase (E.C. 2.7.1.6) Galactokinase is a phosphotransferase that catalyzes the phosphorylation of D-galactose to D-galactose-1-phosphate . At a pH of 7 and temperature of 298 K the apparent equilibrium constant was experimentally measured to be 25 ± 9 [71]. The corresponding standard Gibbs energy change in these conditions, $-7.9 \pm 5.4\ kJ\ mol^{-1}$, is considerably greater than the $-49\ kJ\ mol^{-1}$ standard transformed reaction Gibbs energy back calculated from experimentally measures equilibrium constants, at a temperature of 310.15 K, ionic strength of 0.25 M, and pH of 7.7. The standard transformed reaction Gibbs energy was calculated using the following reactant standard transformed Gibbs energy of formation: ATP = -2188.79, D-Galactose = -336.02, ADP = -1326.02 and alpha-D-Galactose-1-phosphate = -1247.75 , H = 0 ($kJ\ mol^{-1}$). These standard transformed reactant Gibbs energies do not account for the 10 mM concentration of Magnesium ions in the solution when the equilibrium constant of galactokinase was measured. Since ATP is know to bind magnesium ions, a further investigation of this reaction is warranted at constant 10 mM magnesium concentration [29].

γ-glutamyl γ-aminobutyric acid dehydrogenase (puuC) γ-glutamyl γ-aminobutyric acid dehydrogenase catalyzes a key step in the recently discovered putrescine utilization pathway in *E. coli* [72]. Putrescine is an organic polyamine that used as essential cofactor in bacterial ribosomes and is a precursor for spermidine and spermine which are also essential cofactors of ribosomes. Putrescine is also produced by the breakdown of amino acids in living and dead organisms [72]. *E. coli* can catabolise putrescine as the sole nitrogen source in minimal medium, and physiologically this function is used in conditions of nutrient starvation where other more preferable sources of nitrogen are not present. The carbon backbone of putrescine also enters the tricarboxylic acid cycle as succinate. To our knowledge, the equilibrium constant of the γ-glutamyl γ-aminobutyric acid dehydrogenase reaction has not been measured. However, in the unbranched putrescine utilization pathway, the distal reaction, gamma glutamyl putrescine oxidase, is both qualitatively and quantitatively assigned to be irreversible in the forward direction. Therefore the quantitative assignment is consistent with the physiological use of this reaction as an alternate source of nitrogen and carbon.

Glutathione oxidoreductase (E.C. 1.8.1.7) Glutathione oxidoreductase (synonym glutathione reductase), is a member of a flavoproteins family that transfers electrons from a pyridine nucleotide to a specific disulfide containing substrate, in order to maintain the sulfhydryl redox potential in the cytoplasm. Specifically, glutathione oxidoreductase catalyzes the transfer of an electron from NADPH to glutathione disulphide (synonym oxidised glutathione) [73]. In iAF1260, the stoichiometry of this reaction is given as

$$\text{glutathione(oxidized)+h+NADPH} \rightleftharpoons 2 \times \text{glutathione(reduced)+NADP}$$

With this stoichiometry, at 310.15 K, ionic strength 0.25 M, and pH of 7.7, the standard transformed Gibbs energy of the reaction is $-914.0\ kJ\ mol^{-1}$. Although this reaction is experimentally observed to be thermodynamically favourable in the forward direction, this standard transformed Gibbs energy seems excessively large in magnitude. Since Tewari and Goldberg [74] estimated that the apparent equilibrium constant of the reaction is $\simeq 0.013$, giving a standard transformed Gibbs energy of $11.33\ kJ\ mol^{-1}$ at 311.15 K, ionic strength 0.25 M, and pH of 7. The large discrepancy between experimental and back-calculated value seems to originate from the large difference in standard *transformed* Gibbs energy of formation between oxidised and reduced gluthathione (p413 of [30]).

Inosine monophosphate cyclohydrolase (E.C. 3.5.4.10) Inosine monophosphate (IMP) is a precursor in the purine nucleotide *de novo* synthesis pathway, which can either be converted into AMP or GMP. These nucleoside monophosphates are then phosphorylated to produce ATP and GTP. IMP cyclohydrolase catalyzes the cyclization of 5-formamido-1-(5-phospho-D-ribosyl)imidazole-4-carboxamide, eliminating water, to form the imidazole ring of IMP. In iAF1260, this qualitatively reversible reaction was written with IMP as the substrate. With this convention, and using group contribution estimates of reactant standard transformed Gibbs energy, this reaction seems thermodynamically irreversible in the direction written. However, experimentally it was observed that the reverse reaction, synthesis of IMP, is highly favored [75]. At 298 K and pH 7.5, the unidirectional rate constants for the catalytic step were, slower than the observational time for the forward direction $k_f < 1\ s^{-1}$, and much fast for the reverse direction, $40 s^{-1}$, suggesting that the overall reaction is more favorable in the reverse direction, i.e., the production of IMP [75]. Group contribution estimates are derived by estimating a standard Gibbs energy of formation for each of the structural subgroups in a metabolite species. IMP presents a challenge to this method since non-additive effects between subgroups can be expected to be increased in due to the imidazole ring, which is not present in 5-formamido-1-(5-phospho-D-ribosyl)imidazole-4-carboxamide, see Figure 6.

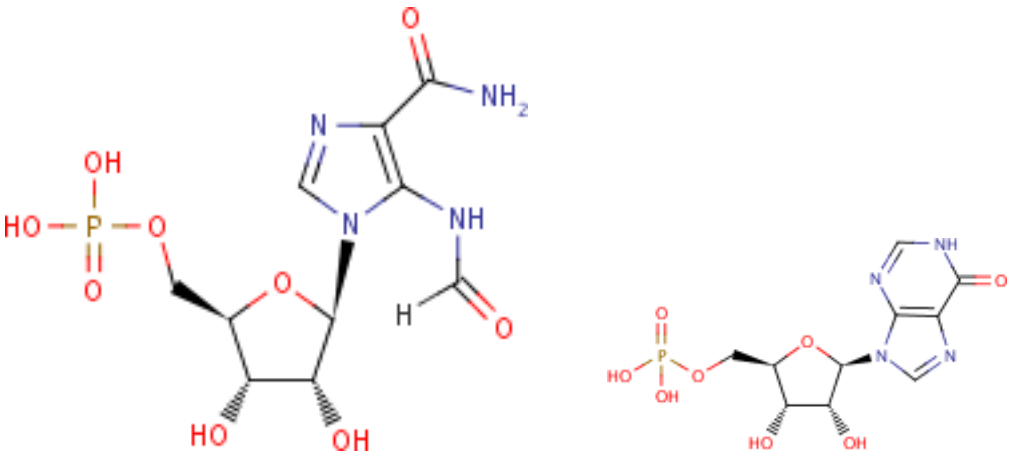

Figure 6: 5-formamido-1-(5-phospho-D-ribosyl)imidazole-4-carboxamide (left) and Inosine monophosphate with the imidazole ring (right) [76].

Phosphoribosylpyrophosphate synthetase (E.C. 2.7.6.1) The biosynthesis of 5-Phospho-alpha-D-ribose-1-diphosphate from alpha-D-Ribose-5-phosphate and ATP is the point at which carbons are drained from the oxidative pentose cycle and utilized for biosynthesis of macromolecular precursors [77]. Thus, this is the first step of a biosynthesis leading to pyrimidine, purine and pyridine as well as histidine. The experimentally measured apparent equilibrium constant was 28.6 [78], at 310 K, pH 7.5 and 5 mM $MgCl_2$. This corresponds to a standard transformed Gibbs energy of -8.64 kJ mol^{-1}, which is significantly different than the estimate of -43.3 kJ mol^{-1} at a temperature of 310.15 K, ionic strength of 0.25 M, and pH of 7.7. The 5-Phospho-alpha-D-ribose-1-diphosphate standard Gibbs energy of formation was estimated using the group contribution method, its structure is illustrated in Figure 7.

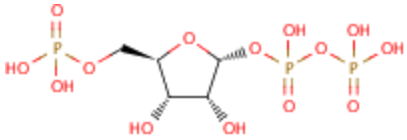

Figure 7: 5-Phospho-alpha-D-ribose-1-diphosphate [76].

A.9.2 Qualitatively reversible yet quantitatively reverse

Phosphate 'reversible' transport via symport periplasm (pitA or pitB) There are two transport mechanisms in *E. coli* for uptake of inorganic phosphate[79]. When periplasmic inorganic phosphate, $pi[p]$, is plentiful, *E. coli* transports it into the cell by a low-affinity, high velocity transport system. The pitA or pitB genes [80, 81] encode this transport system, termed 'Phosphate reversible transport via symport periplasm' in iAF1260. The stoichiometry of this proton symport reaction is assumed to be

$$\text{h[p]+pi[p]} \rightleftharpoons \text{h+pi}$$

and the reaction is assigned to be reversible. At a temperature of 310.15 K, pH of 7.7, and ionic strength of 0.25 M, which are assumed to be identical for both cytoplasm and periplasm, the standard transformed reaction Gibbs energy is 8.5 kJ mol^{-1}. The standard transformed Gibbs energy of the reactants are, $h[p] = 8.68$, $pi[p] = -1062.17$, $h = 0$, $pi = -1045$ kJ mol^{-1}.

The 90 mV electrical potential difference between the cytoplasm and periplasm [53] is responsible for the differences in standard transformed reactant Gibbs energy for these charged metabolites. Various regulatory mechanisms maintain a $8 - 10$ mM cytoplasmic phosphate concentration in various growth conditions [82, 83]. Quantitatively, it seems as if the current 1:1 proton:phosphate stoichiometry is insufficient to facilitate the transport of inorganic

phosphate into the cell, except when periplasmic inorganic phosphate is present at a high concentration, $\gtrsim 0.26\ M$. However, it is known that when the concentration of periplasmic inorganic phosphate is lower than 20 mM, a different high-affinity, low velocity transport system, encoded by pstA/pstB, is induced [84]. Therefore, we predict that either there is a third transport mechanism for uptake of inorganic phosphate, or the proton:phosphate stoichiometry of the low-affinity, high velocity pitA or pitB transporter is 2:1. The latter stoichiometry would give rise to a transformed reactant Gibbs energy of $\sim -2\ kJmol^{-1}$ at a periplasmic inorganic phosphate concentration of 20 mM. However, the caveat is that quantiative prediction of stoichiometry for transport reactions might be altered when non-identical pH and ionic strength for cytoplasm and periplasm are considered.

A.9.3 Qualitatively forward yet quantitatively reverse

Glycogen phosphorylase (E.C. 2.4.1.1) Glycogen is a polysaccharide dendrimer consisting of 12-14 glucose linked in a chain by $\alpha - 1,4$ bonds, chains linked together by $\alpha - 1,6$ branch bonds, see Figure 8. Glycogen phosphorylase, encoded by glgP, is responsible for glyocogenolysis. During extended periods of substrate deprivation, it cleaves $\alpha - 1,4$ bonds releasing one glucose-6-phosphate leaves a chain of the glycogen dendrimer one unit shorter [85]. In iAF1260 this process is represented by the irreversible reaction (GCLP) with the stoichiometry

$$\text{glycogen+pi} \rightarrow \text{D-Glucose1-phosphate}$$

where glycogen represents a single unit in a linear chain of glucose linked by $\alpha - 1,4$ bonds. Implicit in this representation is the fact that in the real reaction the glycogen dendrimer is one unit shorter. In most species, glycogen phosphorylase, cannot cleave a chain with less than 5 glucose units [83]. There is some evidence that this is also the case in *E.coli* [85], therefore the reaction abbreviated GLCP2 involving branched glycogen (bglycogen) seems superfluous.

The equilibrium constant of the glycogenolysis reaction cannot be measured by conventional means since substrate glycogen is indistinguishable from product glycogen [83]. Therefore, it is necessary to measured the reverse reaction, since one can quantify the formation of inorganic phosphate. At pH 7 and 298 K the apparent equilibrium constant for the reaction is 0.28 [83]. This corresponds to a standard transformed Gibbs energy of 3.15 $kJ\ mol^{-1}$. This is markedly different from the quantitative estimate, which uses a group contribution estimate for glycogen. Because the glycogen dendrimer has a variable structure it cannot be accurately represented by a single structure file, complicating group contribution estimation. It has been observed *in vivo* that the glycogen phosphorylase reaction (GLCP) proceeds towards the production of D-Glucose 1-phosphate due to the high concentration of inorganic phosphate, $8 - 10\ mM$, versus D-Glucose 1-phosphate, 170 μM [83]. Therefore, the qualitatively assigned forward direction is correct.

2C-methyl-D-erythritol 2,4-cyclodiphosphate synthase (E.C. 4.6.1.12) Isoprenoids are a large group of organic lipids, which are are all assembled from the universal precursors dimethylallyl diphosphate and isopentenyl diphosphate [86]. To synthesize these precursors, *E. coli* uses an alternate pathway to the mammalian mevalonate pathway, and 2C-methyl-D-erythritol 2,4-cyclodiphosphate synthase catalyzes a step in this alternate pathway. The pathway begins with 1-deoxy-D-xylulose 5-phosphate which is assembled from pyruvate and D-glyceraldehyde 3-phosphate. When isotopically labeled 1-deoxy-D-xylulose was incubated with a recombinant strain engineered for hyperexpression of genes in the non mevalonate pathway, upto and including ispF, coding for 2C-methyl-D-erythritol 2,4-cyclodiphosphate synthase, the ^{13}C nuclear magnetic resonance spectrum of the cell extract was dominated by the known signals of 2C-methyl-D-erythritol 2,4-cyclodiphosphate [86]. While, to our knowledge, the equilibrium constant of the 2C-methyl-D-erythritol 2,4-cyclodiphosphate synthase reaction has not been measured, the aforementioned study indicates that this reaction is correctly qualitatively assigned to be forward, rather than the quantitative assignment of reverse. The substrates and products of the 2C-methyl-D-erythritol 2,4-cyclodiphosphate synthase reaction are significantly structurally distinct which perhaps is a reason for the discrepancy between the quantitative assignment and qualitative assignment of reaction directionality, see Figure 9.

Methionine adenosyltransferase (E.C. 2.5.1.6) Methylation has a myriad of functions in *E. coli* including regulation of gene expression, protein function, and RNA metabolism. Methionine adenosyltransferase catalyzes the synthesis of the most widely uses methy donor, S-adenosylmethionine. The reaction occurs in a two-step reaction, in which the complete tripolyphosphate chain is cleaved from ATP as S-adenosylmethionine is formed, and the tripolyphosphate is further hydrolyzed to pyrophosphate (PPi) and orthophosphate (Pi) [87]. At 298.15 K

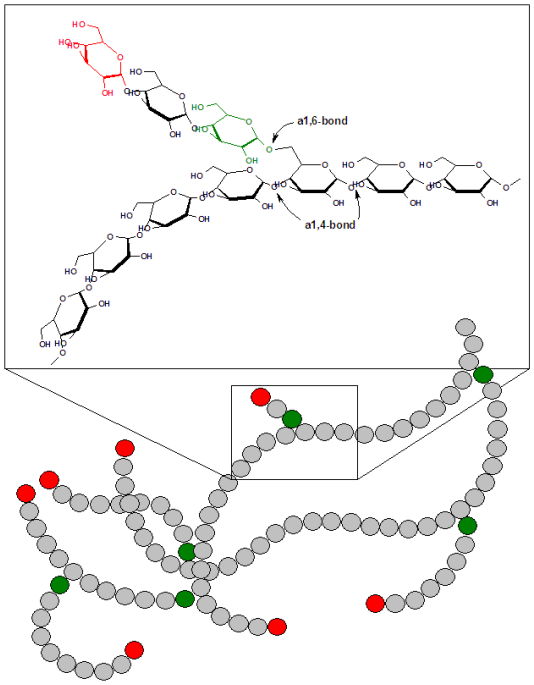

Figure 8: Glycogen

and pH 8, the experimentally measured apparent equilibrium constant was approximately 1×10^4 [88], which corresponds to a standard transformed Gibbs energy of $-23\ kJ\ mol^{-1}$. This conflicts with the positive estimated reaction standard transformed Gibbs energy. At 298.15 K and pH 8, the Gibbs energy profile for the methionine adenosyltransferase reaction was constructed assuming *in vivo* concentrations of ATP (2.6 mM), methionine (0.1 mM), S-adenosylmethionine ($0.08mM$), pyrophosphate (0.5 mM), and orthophosphate (9 mM) [88]. The overall transformed Gibbs energy was $-42\ kJ\ mol^{-1}$ supporting the qualitative assignment of a forward direction for the methionine adenosyltransferase reaction [88].

Phosphoribosylaminoimidazole synthase (E.C. 6.3.3.1) This enzyme catalyzes an intermediate step in de novo purine synthesis, the conversion of 2-Formamido-N1-5-phospho-D-ribosyl-acetamidine (fpram) to 5-amino-1-5-phospho-D-ribosyl-imidazole (air), driven by ATP hydrolysis. At 20 μM ATP & 5 μM 2-Formamido-N1-5-phospho-D-ribosyl-acetamidine, the reaction was experimentally observed to be effectively irreversible in the forward direction [89]. The conversion of 2-Formamido-N1-5-phospho-D-ribosyl-acetamidine to 5-amino-1-5-phospho-D-ribosyl-imidazole, as the name suggests, requires a significant structural rearrangement to form the imidazole ring. Perhaps this is responsible for the erroneous quantitative assignment in this case.

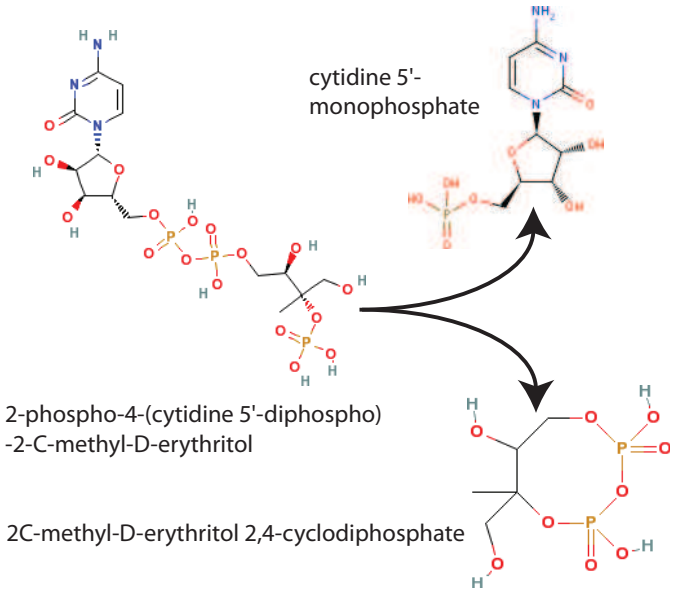

Figure 9: The reaction catalyzed by 2C-methyl-D-erythritol 2,4-cyclodiphosphate synthase, (E.C. 4.6.1.12) [76].

Supplementary Figures

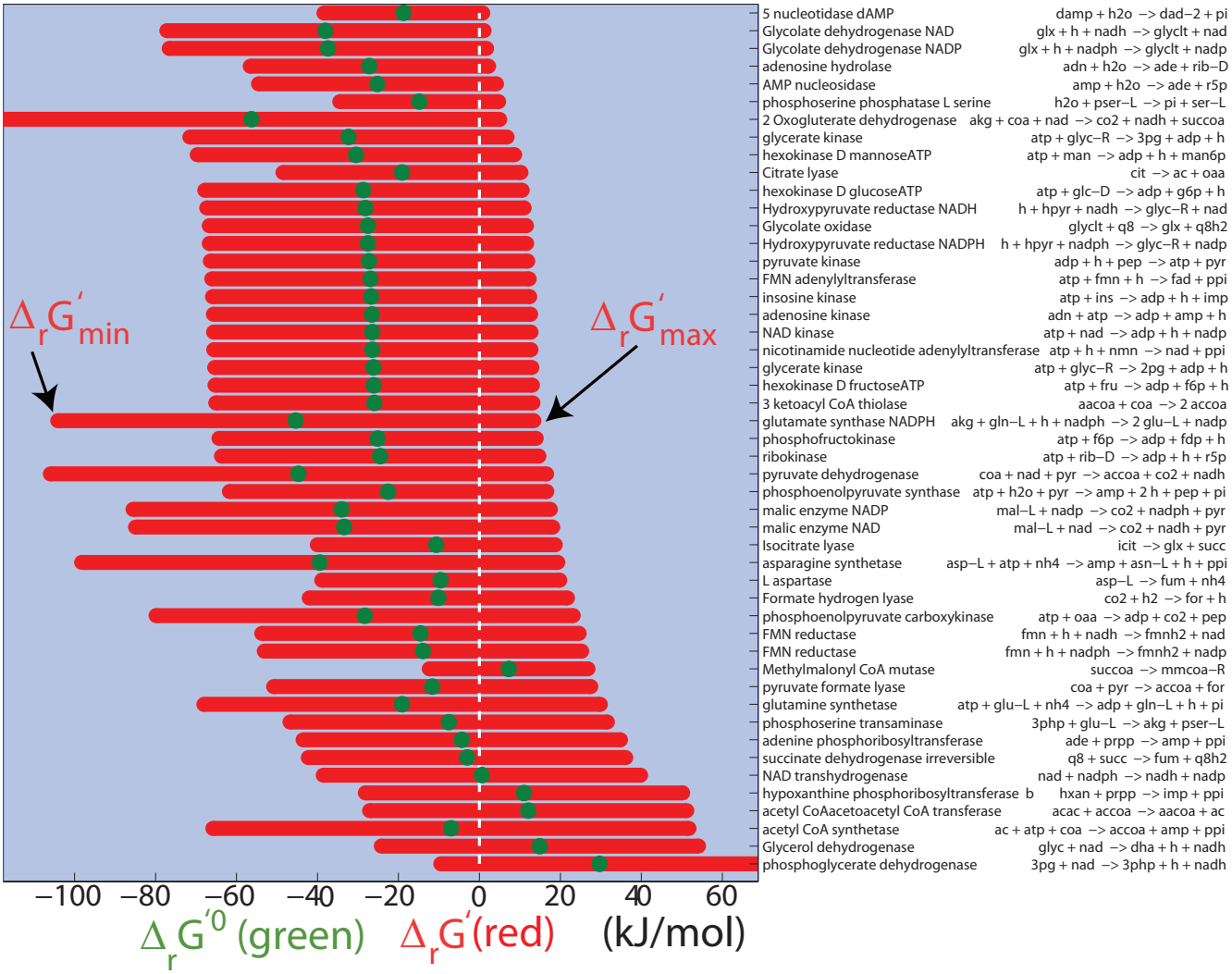

Figure 10: Non transport reactions in iAF1260 which were qualitatively assigned to be forward, yet are quantitatively assigned to be reversible using standard transformed reactant Gibbs energy of formation back calculated from experimentally measured equilibrium constants [30]. Reactions are ordered by ascending maximum transformed reaction Gibbs energy, $\Delta_r G'_{max}$. The reactions towards the bottom are increasingly dependent on higher concentrations of substrates, compared to products, in order to remain quantitatively thermodynamically favorable in the forward direction. We assume a temperature of 310.15 K, ionic strength of 0.25 M, and pH of 7.7 and a physiological range of reactant concentration, $0.01 - 20$ mM, for all reactants, except $[CO_2] = 10^{-4}$ M, $[H_2O] = 1$ M, and $[O_2] = 1 \times 10^{-8} - 8.2 \times 10^{-6}$ M.

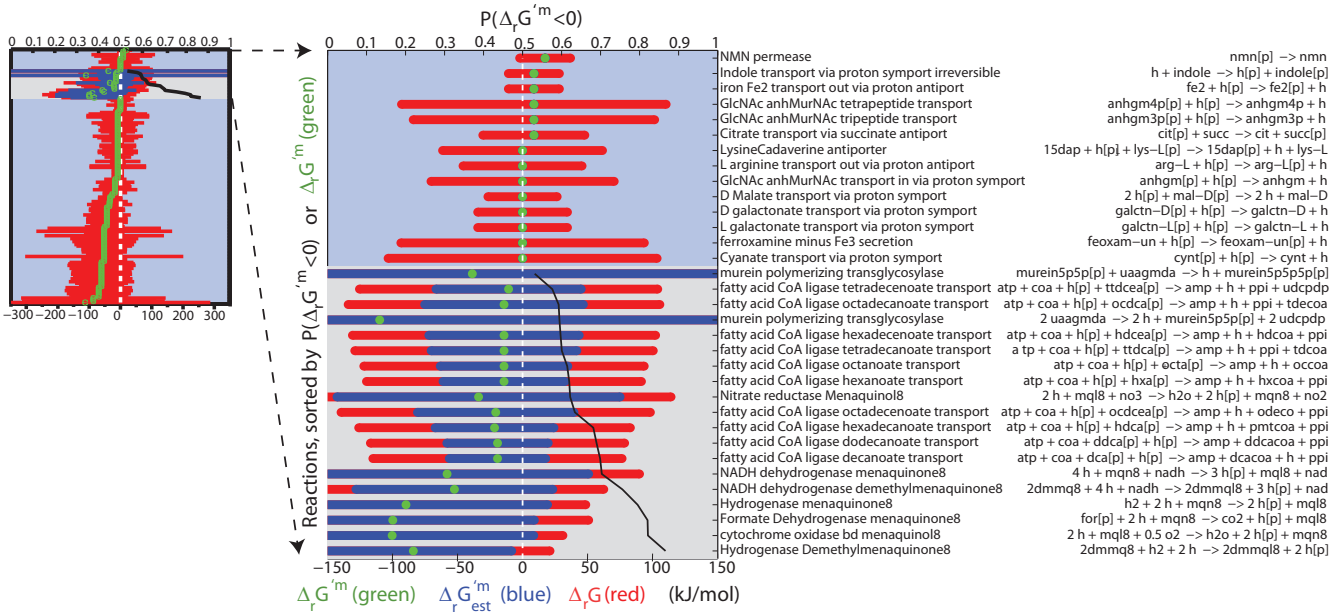

Figure 11: Overview (top left) and zoom (right) of transport reactions which are qualitatively forward, quantitatively reverse, yet required to operate in a forward direction to avoid net shuttling of protons into the periplasmic compartment. Without these reactions qualitatively set to forward, the increased reflux of periplasm protons through the ATP synthase reaction would generate excess ATP, thereby obviating the requirement for oxidative phosphorylation and artificially raising the growth rate. The abbreviatied reaction equations are given for non trivial reactions. The suffix [p] denotes a periplasmic reactant and the remainder of reactants are cytoplasmic. The fatty acid ligase reactions occur less in the periplasm than in the cytoplasmic side of the periplasmic membrane. Representing such spatial details will become more significant when non-identical pH and ioni strength is assumed for cytoplasmic and periplasmic 'compartments'.

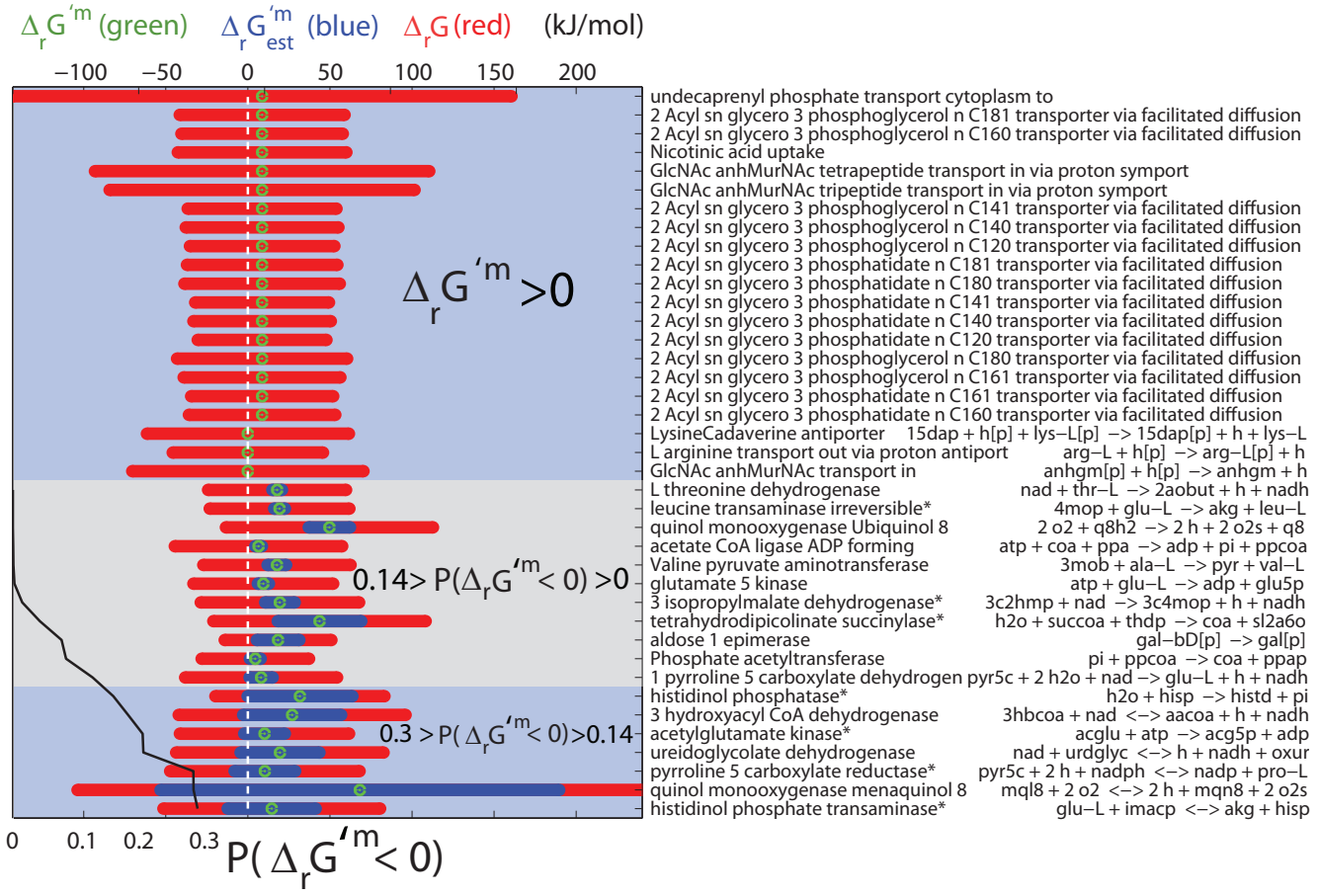

Figure 12: Qualitatively forward reactions that were quantitatively assigned to be reverse in the genome scale *E. coli* model, iAF1260. All reactions either have a positive physiological standard transformed reaction Gibbs energy, $0 < \Delta_r G'^m$, or are below the lower cutoff for cumulative probability of forward physiological standard transformed reaction Gibbs energy, $0.3 \geq P(\Delta_r G'^m < 0)$. Consider the 'nicotinic acid uptake' reaction, which is not coupled to any other thermodynamically favorable reaction in iAF1260. Nicotinic acid is a precursor of the essential coenzymes NAD and NADP. At pH 7, nicotinic acid has a charge of -2, therefore translocation from periplasm to cytoplasm, and accumulation within the cell is predicted to require an energy-dependent process, as has been observed experimentally [90]. The abbreviated reaction Equations are given for non trivial reactions. The suffix [p] denotes a periplasmic reactant and the remainder of reactants are cytoplasmic. It is possible that in vivo reactant concentration may drive any of these reactions in a forward direction. The forward direction of the 7 reactions denoted $*$ are essential for biomass production in glucose minimal medium and were qualitatively set accordingly.

References

[1] B. Ø. Palsson. *Systems Biology: Properties of Reconstructed Networks*. Cambridge University Press, Cambridge, 2006.

[2] I. Thiele and B. Ø. Palsson. A protocol for generating a high-quality genome-scale metabolic reconstruction. *Nat Protoc*, (accepted), 2009.

[3] C. Pál, B. Papp, M. J. Lercher, P. Csermely, S. G. Oliver, and L. D. Hurst. Chance and necessity in the evolution of minimal metabolic networks. *Nature*, 440(7084):667–670, 2006.

[4] R. Mahadevan and C. H. Schilling. The effects of alternate optimal solutions in constraint-based genome-scale metabolic models. *Metab Eng*, 5(4):264–276, 2003.

[5] A. P. Burgard, E. V. Nikolaev, C. H. Schilling, and C. D. Maranas. Flux coupling analysis of genome-scale metabolic network reconstructions. *Genome Res*, 14(2):301–312, 2004.

[6] C. L. Barrett, C. D. Herring, J. L. Reed, and B. Ø. Palsson. The global transcriptional regulatory network for metabolism in *Escherichia coli* exhibits few dominant functional states. *Proc Natl Acad Sci U S A*, 102(52):19103–19108, 2005.

[7] A. Samal and S. Jain. The regulatory network of *E. coli* metabolism as a Boolean dynamical system exhibits both homeostasis and flexibility of response. *BMC Syst Biol*, 2:21, 2008.

[8] J. S. Edwards, R. U. Ibarra, and B. Ø. Palsson. *In silico* predictions of *Escherichia coli* metabolic capabilities are consistent with experimental data. *Nat Biotechnol*, 19(2):125–130, 2001.

[9] R. U. Ibarra, J. S. Edwards, and B. Ø. Palsson. *Escherichia coli* K-12 undergoes adaptive evolution to achieve in silico predicted optimal growth. *Nature*, 420(6912):186–189, 2002.

[10] M. W. Covert, E. M. Knight, J. L. Reed, M. J. Herrgard, and B. Ø. Palsson. Integrating high-throughput and computational data elucidates bacterial networks. *Nature*, 429(6987):92–96, 2004.

[11] M. J. Herrgård, S. S. Fong, and B. Ø. Palsson. Identification of genome-scale metabolic network models using experimentally measured flux profiles. *PLoS Comp Bio*, 2(7):e72, 2006.

[12] J. L. Reed, T. R. Patel, K. H. Chen, A. R. Joyce, M. K. Applebee, C. D. Herring, O. T. Bui, E. M. Knight, S. S. Fong, and B. Ø. Palsson. Systems approach to refining genome annotation. *Proc Natl Acad Sci U S A*, 103(46):17480–17484, 2006.

[13] A. P. Burgard, P. Pharkya, and C. D. Maranas. Optknock: a bilevel programming framework for identifying gene knockout strategies for microbial strain optimization. *Biotechnol Bioeng*, 84(6):647–657, 2003.

[14] K. R. Patil, I. Rocha, J. Förster, and J. Nielsen. Evolutionary programming as a platform for *in silico* metabolic engineering. *BioMed Central Bioinformatics*, 6:308, 2005.

[15] J. H. Park, K. H. Lee, T. Y. Kim, and S. Y. Lee. Metabolic engineering of *Escherichia coli* for the production of L-valine based on transcriptome analysis and *in silico* gene knockout simulation. *Proc Natl Acad Sci U S A*, 104(19):7797–7802, 2007.

[16] A. M. Feist and B. Ø. Palsson. The growing scope of applications of genome-scale metabolic reconstructions using *Escherichia coli*. *Nat Biotechnol*, 26(6):659–667, 2008.

[17] J. M. Savinell and B. O. Palsson. Network analysis of intermediary metabolism using linear optimization. i. development of mathematical formalism. *J Theor Biol*, 154(4):421–454, 1992.

[18] R. Schuetz, L. Kuepfer, and U. Sauer. Systematic evaluation of objective functions for predicting intracellular fluxes in *Escherichia coli*. *Mol Syst Biol*, 3:e119, 2007.

[19] C. S. Henry, M. D. Jankowski, L. J. Broadbelt, and V. Hatzimanikatis. Genome-scale thermodynamic analysis of *Escherichia coli* metabolism. *Biophys J*, 90(4):1453–1461, 2006.

[20] C. S. Henry, L. J. Broadbelt, and V. Hatzimanikatis. Thermodynamics-based metabolic flux analysis. *Biophys J*, 92(5):1792–1805, 2007.

[21] A. Kümmel, S. Panke, and M. Heinemann. Putative regulatory sites unraveled by network-embedded thermodynamic analysis of metabolome data. *Mol Syst Biol*, 2:e34, 2006.

[22] A. Kümmel, S. Panke, and M. Heinemann. Systematic assignment of thermodynamic constraints in metabolic network models. *BioMed Central Bioinformatics*, 7(1):512, 2006.

[23] R.A. Alberty. A short history of the thermodynamics of enzyme-catalyzed reactions. *J Biol Chem*, 279(27):27831–27836, 2004.

[24] K. Burton, H.A. Krebs, and H.L. Kornberg. *Energy Transformations in Living Matter*. Springer-Verlag, Berlin, 1957.

[25] F. Yang, H. Qian, and D. A. Beard. Ab initio prediction of thermodynamically feasible reaction directions from biochemical network stoichiometry. *Metab Eng*, 7(4):251–259, 2005.

[26] Feng Yang and Daniel A Beard. Thermodynamically based profiling of drug metabolism and drug-drug metabolic interactions: a case study of acetaminophen and ethanol toxic interaction. *Biophys Chem*, 120(2):121–134, 2006.

[27] W. J. Heuett and H. Qian. Combining flux and energy balance analysis to model large-scale biochemical networks. *J Bioinform Comput Biol*, 4(6):1227–1243, 2006.

[28] A. M. Feist, C. S. Henry, J. L. Reed, M. Krummenacker, A. R. Joyce, P. D. Karp, L. J. Broadbelt, V. Hatzimanikatis, and B. Ø. Palsson. A genome-scale metabolic reconstruction for *Escherichia coli* K-12 MG1655 that accounts for 1260 ORFs and thermodynamic information. *Mol Syst Biol*, 3(1):e121, 2007.

[29] R. A. Alberty. *Thermodynamics of Biochemical Reactions*. Wiley-Interscience, Hoboken, NJ, 2003.

[30] R. A. Alberty. *Biochemical Thermodynamics: Applications of Mathematica*. Wiley-Interscience, Hoboken, NJ, 2006.

[31] M. D. Jankowski, C. S. Henry, L. J. Broadbelt, and V. Hatzimanikatis. Group contribution method for thermodynamic analysis of complex metabolic networks. *Biophys J*, 95(3):1487–1499, 2008.

[32] M. L. Mavrovouniotis. Estimation of standard Gibbs energy changes of biotransformations. *J Biol Chem*, 266(22):14440–14445, 1991.

[33] A. Varma and B. Ø. Palsson. Metabolic capabilities of *Escherichia coli*: I. Synthesis of biosynthetic precursors and cofactors. *J Theor Biol*, 165(4):477–502, 1993.

[34] A. Varma and B. Ø. Palsson. Stoichiometric flux balance models quantitatively predict growth and metabolic by-product secretion in wild-type *Escherichia coli* W3110. *Appl Environ Microbiol*, 60(10):3724–3731, 1994.

[35] J. Ross. *Thermodynamics and fluctuations far from equilibrium*, volume 80 of *Springer Series in Chemical Physics*. Springer, New York, 2008.

[36] S. Schnell and T. E. Turner. Reaction kinetics in intracellular environments with macromolecular crowding: simulations and rate laws. *Prog Biophys Mol Biol*, 85(2-3):235–260, 2004.

[37] A.P. Minton. How can biochemical reactions within cells differ from those in test tubes? *J Cell Sci*, 119(14):2863, 2006.

[38] A.S. Verkman. Solute and macromolecule diffusion in cellular aqueous compartments. *Trends Biochem Sci*, 27(1):27–33, 2002.

[39] H.P. Kao, J.R. Abney, and A.S. Verkman. Determinants of the translational mobility of a small solute in cell cytoplasm. *J Cell Biol*, 120(1):175–184, 1993.

[40] Esther Biemans-Oldehinkel, Nik A B N Mahmood, and Bert Poolman. A sensor for intracellular ionic strength. *Proc Natl Acad Sci U S A*, 103(28):10624–10629, 2006.

[41] K. A. Dill and S. Bromberg. *Molecular driving forces: Statistical thermodynamics in Chemistry and Biology*. Garland Science, London, 2003.

[42] F. C. Neidhardt (Ed. in Chief), R. Curtis, J. L. Ingraham, E. C. C. Lin, K. B. Low, B. Magasanik, W. S. Reznikoff, M. Riley, M. Schaechter, and H. E. Umbarger (eds). Escherichia coli *and* Salmonella*: Cellular and Molecular Biology*. American Society for Microbiology Press, Washington, DC, 1996.

[43] E. Padan and S. Schuldiner. Intracellular pH and membrane potential as regulators in the prokaryotic cell. *J Membr Biol*, 95(3):189–198, 1987.

[44] J.C. Wilks and J. L. Slonczewski. pH of the cytoplasm and periplasm of *Escherichia coli*: rapid measurement by green fluorescent protein fluorimetry. *J Bacteriol*, 189(15):5601–5607, 2007.

[45] J. L. Slonczewski, R. M. Macnab, J. R. Alger, and A. M. Castle. Effects of pH and repellent tactic stimuli on protein methylation levels in Escherichia coli. *J Bacteriol*, 152(1):384–399, 1982.

[46] W. R. Smith and R. W. Missen. *Chemical Reaction Equilibrium Analysis: Theory and Algorithms*. Wiley, New York, 1982.

[47] A. Fersht. *Structure and mechanism in protein science: A guide to enzyme catalysis and protein folding*. W. H. Freeman, New York, 1999.

[48] O. Fiehn. Metabolomics: the link between genotypes and phenotypes. *Plant Mol Biol*, 48(1-2):155–171, 2002.

[49] M. J. Brauer, J. Yuan, B. D. Bennett, W. Lu, E. Kimball, D. Botstein, and J. D. Rabinowitz. Conservation of the metabolomic response to starvation across two divergent microbes. *Proc Natl Acad Sci U S A*, 103(51):19302–19307, 2006.

[50] N Ishii, K Nakahigashi, T Baba, M Robert, T Soga, A Kanai, T Hirasawa, M Naba, K Hirai, A Hoque, P Y Ho, Y Kakazu, K Sugawara, S Igarashi, S Harada, T Masuda, N Sugiyama, T Togashi, M Hasegawa, Y Takai, K Yugi, K Arakawa, N Iwata, Y Toya, Y Nakayama, T Nishioka, K Shimizu, H Mori, and M Tomita. Multiple high-throughput analyses monitor the response of *E. coli* to perturbations. *Science*, 316(5824):593–597, 2007.

[51] B. D. Bennett, E. H. Kimball, M. Gao, R. Osterhout, S. J. Van Dien, and J. D. Rabinowitz. Absolute metabolite concentrations and implied enzyme active site occupancy in *Escherichia coli*. *Nat. Chem. Biol.*, 5(8):593–9, 2009.

[52] T. Gowers, J. Barrow-Green, and I. Leader. *The Princeton Companion to Mathematics*. Princeton University Pres, Princeton, 2008.

[53] H. Richard and J. W. Foster. *Escherichia coli* glutamate- and arginine-dependent acid resistance systems increase internal pH and reverse transmembrane potential. *J Bacteriol*, 186(18):6032–6041, 2004.

[54] R. A. Alberty. Standard transformed Gibbs energies of coenzyme A derivatives as functions of pH and ionic strength. *Biophys Chem*, 104(1):327–334, 2003.

[55] A. R. Joyce, J. L. Reed, A. White, R. Edwards, A. Osterman, T. Baba, H. Mori, S. A. Lesely, B. Ø. Palsson, and S. Agarwalla. Experimental and computational assessment of conditionally essential genes in *Escherichia coli*? *J Bacteriol*, 188(23):8259–8271, 2006.

[56] J. Yuan, W. U. Fowler, E. Kimball, W. Lu, and J. D. Rabinowitz. Kinetic flux profiling of nitrogen assimilation in *Escherichia coli*. *Nat Chem Biol*, 2(10):529–530, 2006.

[57] H. E. Umbarger. Amino acid biosynthesis and its regulation. *Annu Rev Biochem*, 47:532–606, 1978.

[58] Y.B. Tewari, R.N. Goldberg, and J.D. Rozzell. Thermodynamics of reactions catalysed by branched-chain-amino-acid transaminase. *J Chem Thermodyn*, 32(10):1381–1398, 2000.

[59] A. Varma and B. Ø. Palsson. Metabolic capabilities of *Escherichia coli*: II. Optimal growth patterns. *J Theor Biol*, 165(4):503–522, 1993.

[60] E. Fischer, N. Zamboni, and U. Sauer. High-throughput metabolic flux analysis based on gas chromatography-mass spectrometry derived 13c constraints. *Anal Biochem*, 325(2):308–316, 2004.

[61] J.D. Orth, R.M.T. Fleming, and Bernhard Ø. Palsson. Escherichia coli *and* Salmonella*: Cellular and Molecular Biology*, chapter Reconstruction and use of microbial metabolic networks: the core *Escherichia coli* metabolic model as an educational guide (accepted). ASM Press, 2009.

[62] J. W. Gibbs. *Elementary principles in statistical mechanics, developed with especial reference to the rational foundation of thermodynamics*. Dover Publications, New York, 1902.

[63] R. Baierlein. The elusive chemical potential. *Am J Phys*, 69(4):423–434, 2001.

[64] M. Planck. *Treatise on Thermodynamics*. Courier Dover Publications, Chelmsford, MA, 1945.

[65] R. A. Alberty. IUPAC-IUBMB Joint Commission on Biochemical Nomenclature (JCBN). Recommendations for nomenclature and tables in biochemical thermodynamics. Recommendations 1994. *Eur J Biochem*, 240(1):1–14, 1996.

[66] S. R. Berry, S. A Rice, and J. Ross. *Physical Chemistry*. Oxford University Press, Oxford, 2nd edition, 2000.

[67] R. A. Alberty. Legendre transforms in chemical thermodynamics. *J Chem Thermodyn*, 29(5):501–516, 1997.

[68] Robert A Alberty. The role of water in the thermodynamics of dilute aqueous solutions. *Biophys Chem*, 100(1-3):183–192, 2003.

[69] G. Zhao, A. J. Pease, N. Bharani, and M. E. Winkler. Biochemical characterization of gapb-encoded erythrose 4-phosphate dehydrogenase of *Escherichia coli* k-12 and its possible role in pyridoxal 5'-phosphate biosynthesis. *J Bacteriol*, 177(10):2804–2812, 1995.

[70] S. Boschi-Muller, S. Azza, D. Pollastro, C. Corbier, and G. Branlant. Comparative enzymatic properties of gapb-encoded erythrose-4-phosphate dehydrogenase of escherichia coli and phosphorylating glyceraldehyde-3-phosphate dehydrogenase. *J Biol Chem*, 272(24):15106–15112, 1997.

[71] M. R. Atkinson, E. Johnson, and R. K. Morton. Equilibrium constant of the galactokinase reaction and free energy of hydrolysis of adenosine triphosphate. *Nature*, 184:1925–1927, 1959.

[72] S. Kurihara, S. Oda, K. Kato, H. G. Kim, T. Koyanagi, H. Kumagai, and H. Suzuki. A novel putrescine utilization pathway involves gamma-glutamylated intermediates of *Escherichia coli* k-12. *J Biol Chem*, 280(6):4602–4608, 2005.

[73] K.G. Knapp and J. R. Swartz. Cell-free production of active *E. coli* thioredoxin reductase and glutathione reductase. *FEBS Lett*, 559(1-3):66–70, 2004.

[74] Y.B. Tewari and R.N. Goldberg. Thermodynamics of the oxidation–reduction reaction {2 glutathionered (aq)+ NADPox (aq)= glutathioneox (aq)+ NADPred (aq)}. *J Chem Thermodyn*, 35(8):1361–1381, 2003.

[75] K. G. Bulock, G. P. Beardsley, and K. S. Anderson. The kinetic mechanism of the human bifunctional enzyme atic (5-amino-4-imidazolecarboxamide ribonucleotide transformylase/inosine 5'-monophosphate cyclohydrolase). a surprising lack of substrate channeling. *J Biol Chem*, 277(25):22168–22174, 2002.

[76] K. Degtyarenko, P. de Matos, M. Ennis, J. Hastings, M. Zbinden, A. McNaught, R. Alcántara, M. Darsow, M. Guedj, and M. Ashburner. ChEBI: a database and ontology for chemical entities of biological interest. *Nucleic Acids Res*, 36(Database issue):D344–D350, 2008.

[77] M. Willemos and B. Hove-Jensen. Binding of divalent magnesium by *Escherichia coli* phosphoribosyl diphosphate synthetase. *Biochemistry*, 36(16):5078–5083, 1997.

[78] R. L. Switzer. Regulation and mechanism of phosphoribosylpyrophosphate synthetase. i. purification and properties of the enzyme from *Salmonella typhimurium*. *J Biol Chem*, 244(11):2854–2863, 1969.

[79] A. K. White and W. W. Metcalf. Microbial metabolism of reduced phosphorus compounds. *Annu Rev Microbiol*, 61:379–400, 2007.

[80] G. R. Willsky and M. H. Malamy. Characterization of two genetically separable inorganic phosphate transport systems in *Escherichia coli*. *J Bacteriol*, 144(1):356–365, 1980.

[81] R. M. Harris, D. C. Webb, S. M. Howitt, and G. B. Cox. Characterization of PitA and PitB from *Escherichia coli*. *J Bacteriol*, 183(17):5008–5014, 2001.

[82] N. Amin and A. Peterkofsky. A dual mechanism for regulating cAMP levels in *Escherichia coli*. *J Biol Chem*, 270(20):11803–11805, 1995.

[83] T. Traut. *Allosteric Regulatory Enzymes*. Springer Verlag, 2007.

[84] N. N. Rao and A. Torriani. Molecular aspects of phosphate transport in *Escherichia coli*. *Mol Microbiol*, 4(7):1083–1090, 1990.

[85] N. Alonso-Casajús, D. Dauvillée, A. M. Viale, F. J. Muñoz, E. Baroja-Fernández, M. T. Morán-Zorzano, G. Eydallin, S. Ball, and J. Pozueta-Romero. Glycogen phosphorylase, the product of the glgp gene, catalyzes glycogen breakdown by removing glucose units from the nonreducing ends in *Escherichia coli*. *J Bacteriol*, 188(14):5266–5272, 2006.

[86] S. Hecht, W. Eisenreich, P. Adam, S. Amslinger, K. Kis, A. Bacher, D. Arigoni, and F. Rohdich. Studies on the nonmevalonate pathway to terpenes: the role of the gcpe (ispg) protein. *Proc Natl Acad Sci U S A*, 98(26):14837–14842, 2001.

[87] J. Komoto, T. Yamada, Y. Takata, G. D. Markham, and F. Takusagawa. Crystal structure of the s-adenosylmethionine synthetase ternary complex: a novel catalytic mechanism of s-adenosylmethionine synthesis from atp and met. *Biochemistry*, 43(7):1821–1831, 2004.

[88] M. S. McQueney, K. S. Anderson, and G. D. Markham. Energetics of s-adenosylmethionine synthetase catalysis. *Biochemistry*, 39(15):4443–4454, 2000.

[89] J. L. Schrimsher, F. J. Schendel, J. Stubbe, and J. M. Smith. Purification and characterization of aminoimidazole ribonucleotide synthetase from *Escherichia coli*. *Biochemistry*, 25(15):4366–4371, 1986.

[90] J. J. Rowe, R. D. Lemmon, and G. J. Tritz. Nicotinic acid transport in *Escherichia coli*. *Microbios*, 44(179-180):169–184, 1985.